

## USE OF X-RAY TRANSMISSION DIFFRACTOMETRY FOR THE STUDY OF CLAY-PARTICLE ORIENTATION AT DIFFERENT WATER CONTENTS

A.C. IÑIGO,<sup>1</sup> D. TESSIER,<sup>2</sup> AND M. PERNES<sup>2</sup>

<sup>1</sup>IRNA, Cordel de Merinas 40-52, 37008 Salamanca, Spain

<sup>2</sup>INRA, Science du Sol, 78026 Versailles, France

**Abstract**—Homoionic Ca-saturated clay pastes were prepared and drying curves were obtained by applying suction pressures from 1 kPa to 100 MPa. A transmission device was used to study particle orientation by placing the clay in a cell specially designed to obtain diagrams corresponding to different sample orientations. The  $00l$  and  $hk0$  reflections were compared to determine the best reflections for studying clay-particle orientation. Depending on the clay,  $00l$  reflections or the  $020$  reflection and/or  $hkl$  bands can be used to analyze orientation. In many cases the  $020$  reflection is preferred because the intensity of the peak is high and appears to be independent of the  $H_2O$  content and the degree of stacking order of layers along the  $[001]$  direction.

For interstratified clays, the conditions required to obtain  $00l$  reflections depended on several factors, the most important of which is the water content. Also, the intensity relating to particle orientation depends on (1) particle extension (size) in the  $(00l)$  plane and (2) the crystal structure. Illite crystals of  $<1000$  Å gave a poorly oriented clay matrix. In contrast, large aggregates of illite, smectite, and kaolinite particles ( $>10,000$  Å) showed a strongly oriented system. The particles of smectites may be curved and the dry material was poorly oriented owing to weak cohesion forces between the layers in comparison to illite.

The study of the orientation of particles by X-ray diffraction on hydrated samples may be affected by sample mounting techniques. Any change in the content or the way the sample is mounted may modify the microstructure of a material.

Clay containing a high water content affects the disorientation of particles, whereas, for the dry samples, pore size, pore volume, and solid continuity are associated with the geometry and crystal structure of the clay matrix.

**Key Words**—Clay, Hydration, Illite, Microstructure, Particle Orientation, Smectite, Transmission X-ray Diffraction.

### INTRODUCTION

Clays are finely divided solids, which present a large reaction surface and which interact strongly with water. At high water contents, water extraction from a clay usually induces a decrease in volume, *i.e.*, a shrinkage which produces a compaction of the sample. Conversely, water absorption often leads to swelling even at very low-energy levels, *i.e.*, suction pressures of  $\sim 1$  kPa (Méring, 1946; Norrish, 1954; Aylmore and Quirk, 1959; Tessier, 1978a, 1984). Each stage of shrinkage and swelling has different rheological and mechanical properties. In soils, for example, volume variations lead to macroscopic discontinuities, such as cracks and shear planes (Wilding and Tessier, 1988; Tessier *et al.*, 1992).

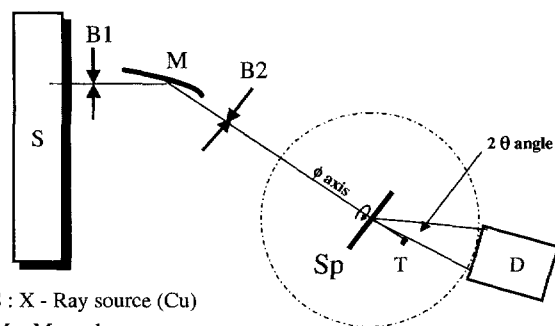
The change in clay volume involves a complex mechanism and variations in the interlayer distance are primarily involved (Méring, 1949; Norrish, 1954; Aylmore and Quirk, 1959). However, this alone cannot explain shrinkage/swelling properties. Whatever the clay, a large portion of the water fills much larger spacings than those involving the interlayer, corresponding to intercrystallite spacings and interaggregate pores. The presence of these different types of organization (*i.e.*, interlayer, interparticle spacings, and interaggregate pores) explains numerous macroscopic

properties. In addition to swelling/shrinkage, water-transfer and rheological properties are affected (Assouline *et al.*, 1997).

An analysis of the various particle arrangements and their respective contribution to properties is required to understand and model clay properties. Taylor and Norrish (1966) used X-ray diffraction to study the orientation of kaolinite crystallites. Tessier (1978b) developed a similar technique to study samples of various clays with different moisture contents. To analyze the orientation of clay particles by X-ray diffraction, the oblique-diffraction technique has been used also (Mamy, 1975; Wiewiora, 1982). This article presents developments in X-ray transmission diffractometry to study the clay organization during drying.

### ADVANTAGES OF X-RAY TRANSMISSION DIFFRACTOMETRY

X-ray diffraction is used routinely to identify soil and deposit minerals. In practice, for very well-oriented films, the intensity of reflections in a given orientation may vary considerably, ranging from increasing greatly or disappearing (Plançon, 1980; Courville *et al.*, 1979). The advantage of an X-ray transmission device is that the incidence angle may be selected to obtain the maximum intensity for a given reflection, *i.e.*, either  $00l$  or  $hkl$ . Thus the preferential orientation



S : X - Ray source (Cu)  
 M : Monochromator  
 (curved crystal of Ge)  
 B1 , B2 : Slits  
 Sp : Rotating sample holder  
 T : Trap  
 D : Position of Detector

Figure 1. Diagram of the X-ray transmission device.

angle of the sample can be calculated to obtain the maximum intensity for a given family of planes (Wiewiora and Weiss, 1985).

Adsorption is not negligible in the transmission method. The resultant intensity requires correction relating to the irradiated mass of the solid to obtain optimal diffraction conditions. According to Wiewiora and Weiss (1985), the amount of irradiated clay for this device is  $\sim 0.02\text{--}0.03\text{ g cm}^{-2}$  for either 1:1 or 2:1 phyllosilicates. For a water content of  $\sim 500\%$  (mass of water/mass of solid  $\times 100$ ), the dry bulk density is  $\sim 0.2\text{ g cm}^{-3}$ . To obtain optimal diffraction conditions, the irradiated section should be 1 mm thick. Note that the irradiated volume and the reflection intensity depend on the value of the  $\theta$  incident angle. For  $1^\circ < \theta < 10^\circ$ , *i.e.*, for 001, 002, and 020 reflections of 2:1 phyllosilicates and kaolinite, the volume irradiated by the X-ray beam remains nearly constant.

Choosing either a 00 $l$  reflection or the 020 reflection for examination depends on the clay organization. The height of a 001 peak in clays depends on the size of the coherent domains (Brindley, 1980; Reynolds,

1980; Plançon, 1980; Nadeau *et al.*, 1984) and on the regularity of the interlayer distances (Pons *et al.*, 1981). For highly hydrated samples, such as those studied here, the regularity of distances depends primarily on the type of exchangeable cations and the energy range of the water in contact with the clay (suction pressure and salt concentration of the solution) (Norrish, 1954; Ben Rhaïem *et al.*, 1987). The choice of a transmission device involves the nature of the clay type, the ionic environment, and the energy range of water studied. For smectite pastes prepared with a divalent cation, such as Ca and Mg, interlayer spacings are mostly limited to three H<sub>2</sub>O layers, even for very hydrated clay pastes (Tessier, 1984).

## METHODS

### X-ray transmission device

To study the orientation of the samples, a Siemens D-5000 diffractometer was used with CuK $\alpha$  radiation. The K $\alpha_1$  radiation was isolated using a germanium monochromator. Soller slits and a divergence slit were placed between the X-ray source and the sample to obtain data at low angles ( $2\theta = \sim 1.0^\circ$ ). A linear detector covering a range of  $2\theta = 12^\circ$  was used, the sample holder is perpendicular to the X-ray source and may rotate about the  $\phi$  axis from  $0^\circ$  to  $360^\circ$  (Figure 1). We generally made X-ray patterns every  $10^\circ$ .

The sample was a slice a few micrometers thick. Because the sample rotated about  $\phi$ , the irradiated volume was constant for a given diffraction peak whatever the rotation angle. The sample-holder design ensured that there was no contact between the sample and the ambient air to avoid drying during the study. The design utilizes two mica windows sealed with epoxy to allow X-ray transmittance. The windows delimited an enclosure with a volume of  $\sim 0.15\text{ cm}^3$ . The sample was introduced through an external window and an O-ring ensured the device was airtight. The mica windows did not produce any detectable diffraction peaks.

### Samples

Six clays from soils and deposit clays were selected (see Tessier and Pédro, 1976; Tessier, 1978a, 1984; Vasseur *et al.*, 1995, Iñigo and Tessier, 1996). For the soil clays, organic matter was removed by H<sub>2</sub>O<sub>2</sub> treatment (Kunche and Rich, 1959). For the clay from La Bouzule, a small amount of carbonate was removed by treatment with a mixture of Na acetate and acetic acid (Grossman and Millet, 1961). For the Wyoming montmorillonite and the Saint Austell kaolinite, we studied the  $<2\text{-}\mu\text{m}$  size fraction, whereas for the soil clays, several fractions were studied, *i.e.*, 0–0.2 and 0.2–2  $\mu\text{m}$  for the Salins illite, and 0.02–2 and 2–5  $\mu\text{m}$  for the La Bouzule clay.

Table 1 shows the cation-exchange capacity and the specific surface area of the studied clays. X-ray dif-

Table 1. Total chemical analyses, cation-exchange capacity (CEC), and EGME surface area of clay fractions of the soils and deposit clays studied.

Sample	<sup>1</sup> CEC	<sup>2</sup> EGME S.A.
Wyoming montmorillonite	87.1	719
Illite-smectite, kaolinite		
La Bouzule (0.2–2)	31.0	249
Illite-smectite, kaolinite		
La Bouzule (2–5)	31.4	249
Salins illite (0–0.2)	30.9	373
Salins illite (0.2–2)	25.9	303
St. Austell kaolinite	1.4	11

<sup>1</sup> Cation-exchange capacity in cmol kg<sup>-1</sup>.

<sup>2</sup> Total surface area, based on the retention of ethylene glycol monoethyl ether in m<sup>2</sup>/g.

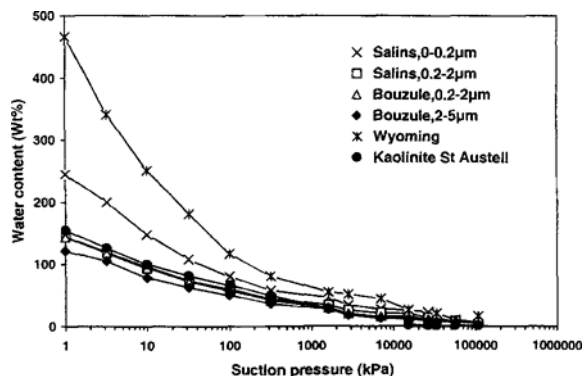


Figure 2. Water retention curves of clays.

fractometry showed that the  $d(001)$  value of the Carich montmorillonite was 15.6 Å (smectite) at 50% relative humidity. The mineralogical data for the other clays are presented in Djéran-Maigre *et al.* (1998). In the Salins illite, all fractions show 10-Å layer spacings confirming illite. La Bouzule clay fractions were identified as an interstratified illite-smectite clay with ~15 and 10-Å layer spacings and a small amount of very low-defect kaolinite (~10%). In the Saint Austell kaolinite, a 7.14-Å layer spacing was observed confirming kaolinite, but the clay contained a very small amount of mica (10-Å peak).

The clay fraction of the Wyoming smectite has the largest specific surface area and that of the Saint Austell kaolinite the smallest. La Bouzule clay fractions have a specific surface area slightly smaller than those of Salins, and both surface areas are intermediate between those of kaolinite and smectite. The cation-exchange capacities were similar in the granulometric fractions of the Salins and La Bouzule samples.

In our experiments, clays were first saturated with calcium ions following Robert and Tessier (1974). Clays with varying water content were prepared as paste and homogenized by mechanical stirring. They were then subjected to suction pressure varying from 1 kPa to 100 MPa, obtained by using a filtration device for pressures of  $\leq 1.6$  MPa or obtained by contact with vapor pressures for pressures  $> 1.6$  MPa (Tessier, 1978a). After equilibrium was reached, materials acquired sufficient cohesion to section with a thin steel wire (~50  $\mu\text{m}$ ). Thin rectangular slices of clay paste were obtained with a homogeneous thickness and very few perturbations to their surfaces (Tessier, 1978b). These slices were placed into the sample holder so that the direction of the suction pressure applied was perpendicular to the direction of the incident X-ray beam. In the sample holder, the reference orientation plane was that of the pressure cell. The total counting time was 4000 s for each pattern.

Clay minerals tend to orient in a direction parallel to the sample holder in which the samples are dried.

When the samples loses water, the intensity of the  $00l$  reflections varies. In clay minerals, the 001, 002, or 003 bands as well as an  $hkl$  band, such as the 020 reflection, can be used. When clay is interstratified or contains a mixture of several mineral species, such as the La Bouzule sample, we selected the 001 reflection of the mineral with the highest proportion (kaolinite) as well as the 020 reflection corresponding to each clay. The transmission device does not make it possible to obtain patterns at high angles, and thus the 060 reflection was not examined.

To interpret these results, we compared the patterns obtained at different water contents for each day and compared these results to each other. The latter was done by normalizing diagrams, *i.e.*, by multiplying the area of each diffraction peak by an appropriate factor to obtain orientation curves with an identical area over  $\phi$  rotations of 180°. For each clay, the surface area of the orientation curve was constant even if the shape of the curve varied.

#### Transmission electron microscopy studies

Transmission electron microscopy (TEM) was performed on samples prepared at 1-kPa suction pressure. The method consists of embedding the samples in epoxy with their initial degree of humidity following Tessier (1984) and Kim *et al.* (1995). Each clay sample is placed in contact with methanol to replace the interstitial solution. Methanol is miscible with propylene oxide, which is miscible also with the different components of Spurr's resin. Under humid conditions, the solvents penetrate both the very small pores and the clay interlayer, thereby making it possible to distinguish clay species (Tessier, 1984; Elsass *et al.*, 1998). After sectioning with an ultramicrotome, TEM imaging was obtained with a Philips 420 STEM microscope operating at 120 kV. Magnification ranged from 3000 to 51,000 and high resolution lattice-fringe images were obtained.

## RESULTS

#### Water and volume change

Water content was obtained on many suction pressures ranging from 1 kPa to 100 MPa. Figure 2 indicates that most of the water in clays was lost between 1 kPa and 1 MPa. In this range, water content decreased as follows: Wyoming  $>$  Salins (0–0.2  $\mu\text{m}$ )  $>$  Salins (0.2–2  $\mu\text{m}$ )  $\approx$  La Bouzule  $\approx$  Saint Austell. Note that, for a given clay, particle size had little effect on water retention, especially for the La Bouzule clay.

The change in clay volume was deduced from water-retention curves (Tessier, 1984). For suction pressures of  $\leq 1$  MPa, clays with fine particles, such as illites and smectites, are saturated with water. We can thus assert that, during drying, the change in volume was equal to water loss and that variations in water

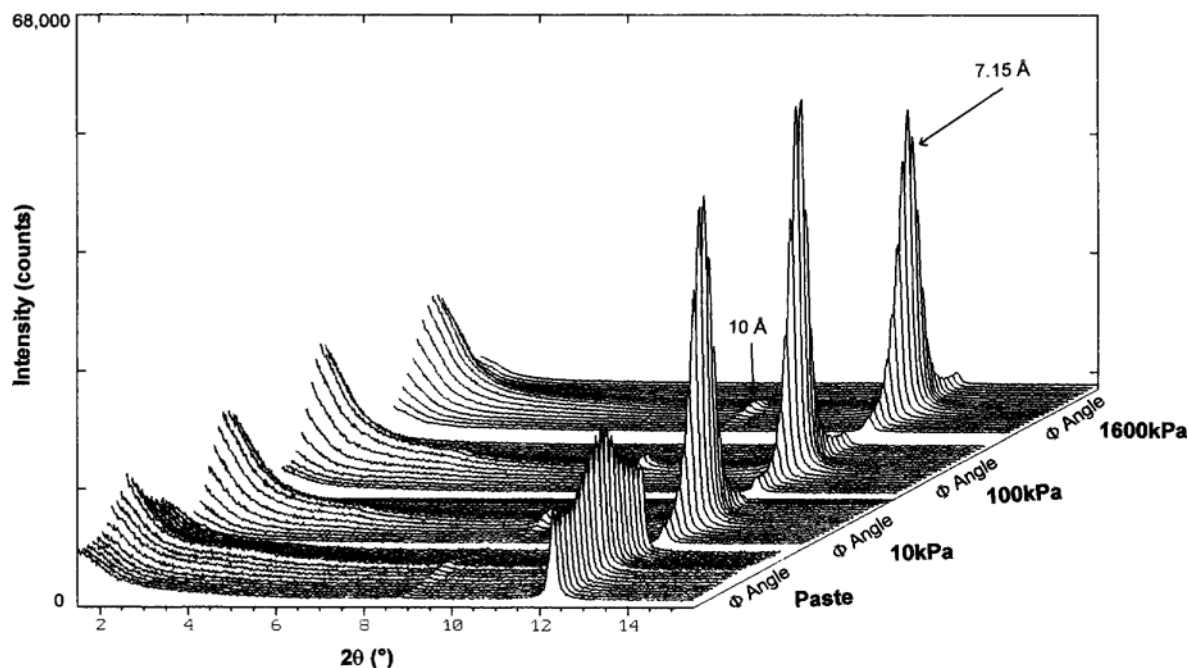


Figure 3. X-ray orientation patterns obtained on the Saint Austell kaolinite on paste and for 10, 100, and 1600 kPa suction pressures.

content consequently reflect volume variations (Tessier, 1984).

#### Particle orientation

**Saint Austell kaolinite.** Four series of patterns are presented in Figure 3. In the initial paste, water content was near 600% and progressively decreased at 10 kPa, 100 kPa, and 1.6 MPa. At each suction pressure, 19 patterns corresponding to rotation angles of  $10^\circ$  at intervals from  $0^\circ$  to  $180^\circ$  are presented for  $2\theta = 1.5\text{--}14.5^\circ$ .

In the initial paste, the patterns show that intensities vary as a function of rotation angle,  $\phi$ , of the sample. For the 001 reflection, maximum intensity was obtained from  $70^\circ$  to  $110^\circ$ . In this angle range, particles are preferentially oriented towards the sample holder ( $\sim \pm 20^\circ$ ). During drying, the phenomenon amplified. For the 001, the differences in intensity between the central part of the curve ( $70\text{--}110^\circ$ ) and the wide orientation angles ( $0\text{--}70^\circ$  and  $110\text{--}180^\circ$ ) were considerable. We conclude that particles strongly orient at  $\leq 100$  kPa. Orientation effects then slightly decreased, which signifies a small global disorientation of particles at 1.6 MPa in comparison to 100 kPa.

**Salins illite.** Patterns were obtained with size fractions of  $<0.2$  and  $0.2\text{--}2$   $\mu\text{m}$ . The results of size fraction of  $<0.2$   $\mu\text{m}$  are reported in Figure 4. The patterns corresponding to the 001 reflection were obtained under the same conditions as for Saint Austell kaolinite (paste, 10, 100, and 1.6 MPa) and in the same angle

range. The intensity of the 001 reflection from illite is much lower and broader than that from Saint Austell kaolinite. Given the specific surface area of these two clays, *i.e.*, 11 and 373  $\text{m}^2 \text{g}^{-1}$ , respectively, the size of the coherent domains is probably much smaller in illite than in kaolinite. In contrast to kaolinite, particles of illite were not oriented in the initial paste. Clay orientation increased with increasing pressures. The results obtained in the  $0.2\text{--}2\text{-}\mu\text{m}$  size fraction were identical and are thus not presented here.

**La Bouzule.** The patterns in Figures 5 and 6 involve the  $0.2\text{--}2$  and  $2\text{--}5\text{-}\mu\text{m}$  size fractions, respectively. Unlike other clays, the initial paste did not allow identification of the 001 and 002 peaks for kaolinite, illite, and smectite. The 020 reflection at 4.47  $\text{\AA}$  and the quartz reflection at 4.26  $\text{\AA}$  are clearly observed. Unlike other clays, the initial paste did not allow identification of the 001 and 002 peaks for kaolinite and interstratified I-S.

At a suction pressure of 10 kPa in the  $0.2\text{--}2\text{-}\mu\text{m}$  size fraction, the 001 reflection of kaolinite and the 002 reflection of illite are clearly present (Figure 5). For the  $2\text{--}5\text{-}\mu\text{m}$  size fraction, 001 reflections are absent (Figure 6). In both fractions, the intensity of the 020 reflection at 4.47  $\text{\AA}$  increased between  $0\text{--}40^\circ$  and  $140\text{--}180^\circ$ , *i.e.*, for large orientation angles. Note that the quartz reflection at 4.26  $\text{\AA}$  did not depend on clay orientation.

From 100 kPa, the 001 peak of kaolinite appeared in the  $2\text{--}5\text{-}\mu\text{m}$  size fraction (Figure 6). The intensity

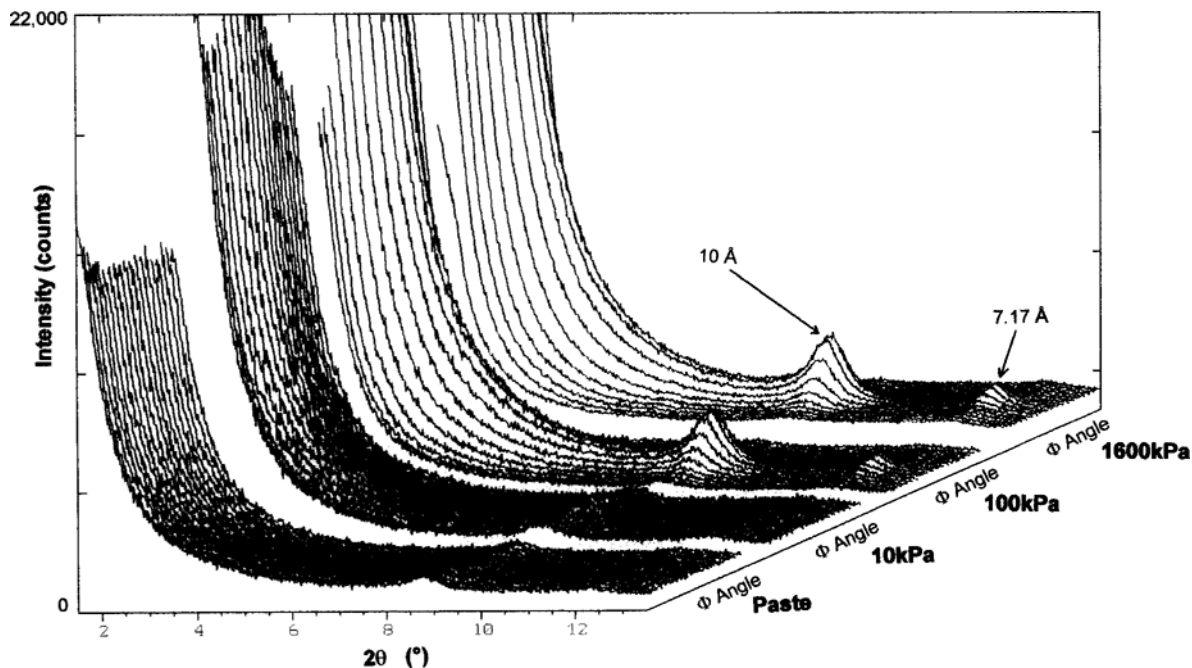


Figure 4. X-ray orientation patterns obtained on the Salins illite on the size fraction of  $<0.2 \mu\text{m}$  (paste) and for 10, 100, and 1600 kPa suction pressures.

of the 001 peak progressively increased as suction pressure increased to 1.6 MPa. Note also that the 001 reflection of kaolinite decreased as the 020 reflection increased. Figure 7 shows intensity variations according to the rotation angle obtained at 100 kPa.

*Wyoming montmorillonite*. As with kaolinite and Salins illite, the 001 peak is observed in the initial paste and in a suction-pressure range from 1 kPa to 1.6 MPa (Figure 8). The diffraction peak is located at  $\sim 19.0 \text{ \AA}$  and did not vary in this pressure range. The orientation

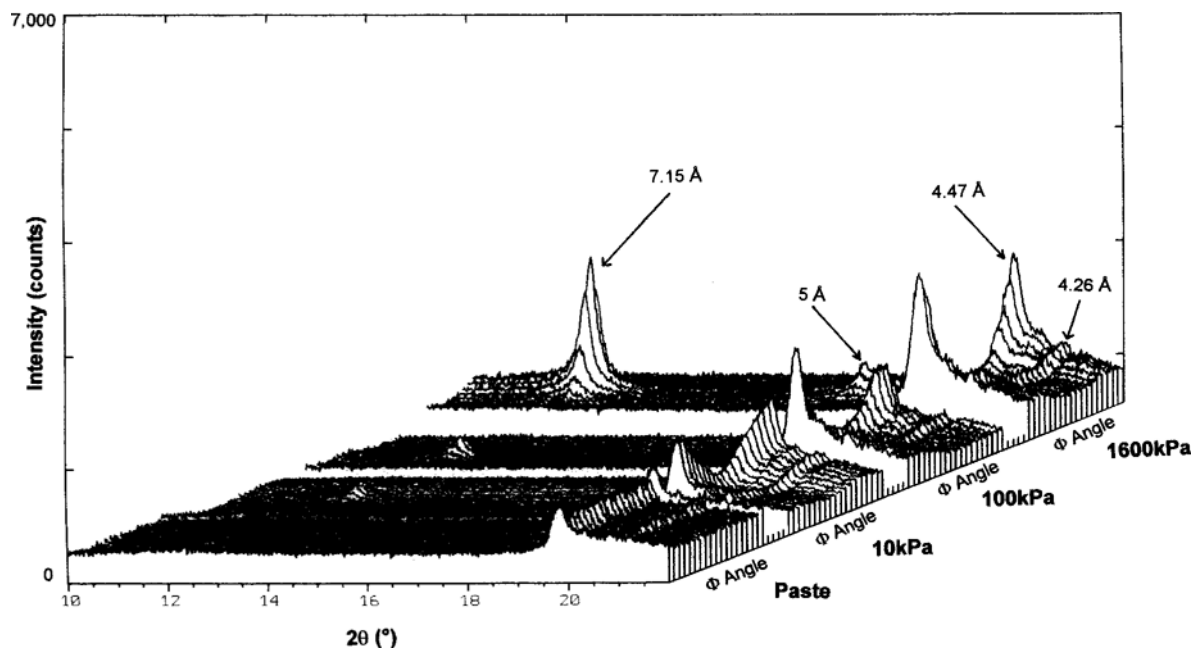


Figure 5. X-ray orientation patterns obtained on the size fraction of  $0.2\text{--}2 \mu\text{m}$  of the La Bouzule clay on paste and for 10, 100, and 1600 kPa suction pressures.

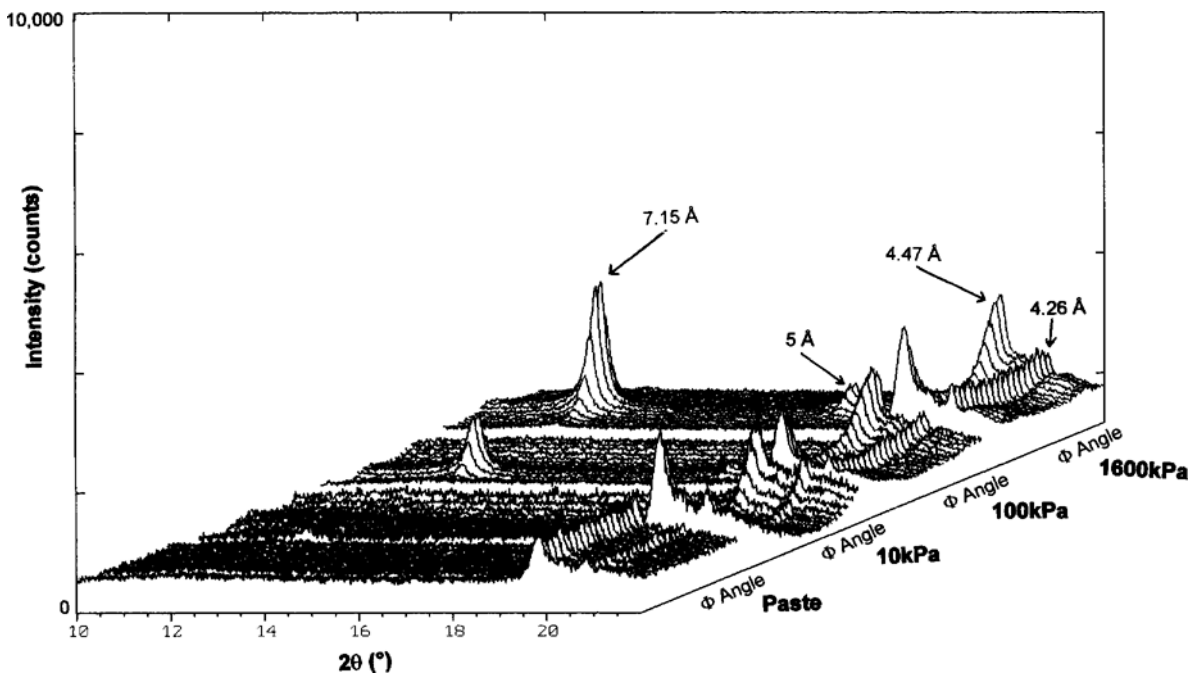


Figure 6. X-ray orientation patterns obtained on the size fraction of 2–5 μm of the La Bouzule clay on paste and for 10, 100, and 1600 kPa suction pressures.

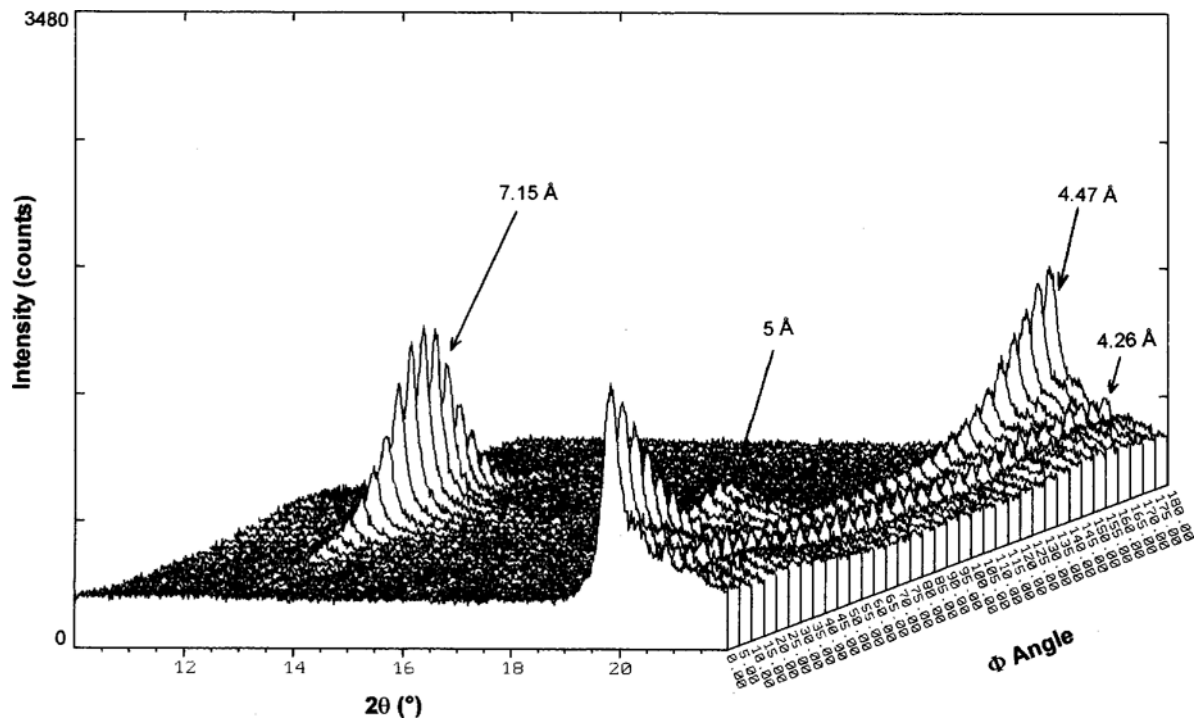


Figure 7. Comparison of the X-ray orientation patterns for 001 and 020 reflections of the La Bouzule sample (0.2–2 μm) at 100 kPa suction pressures.

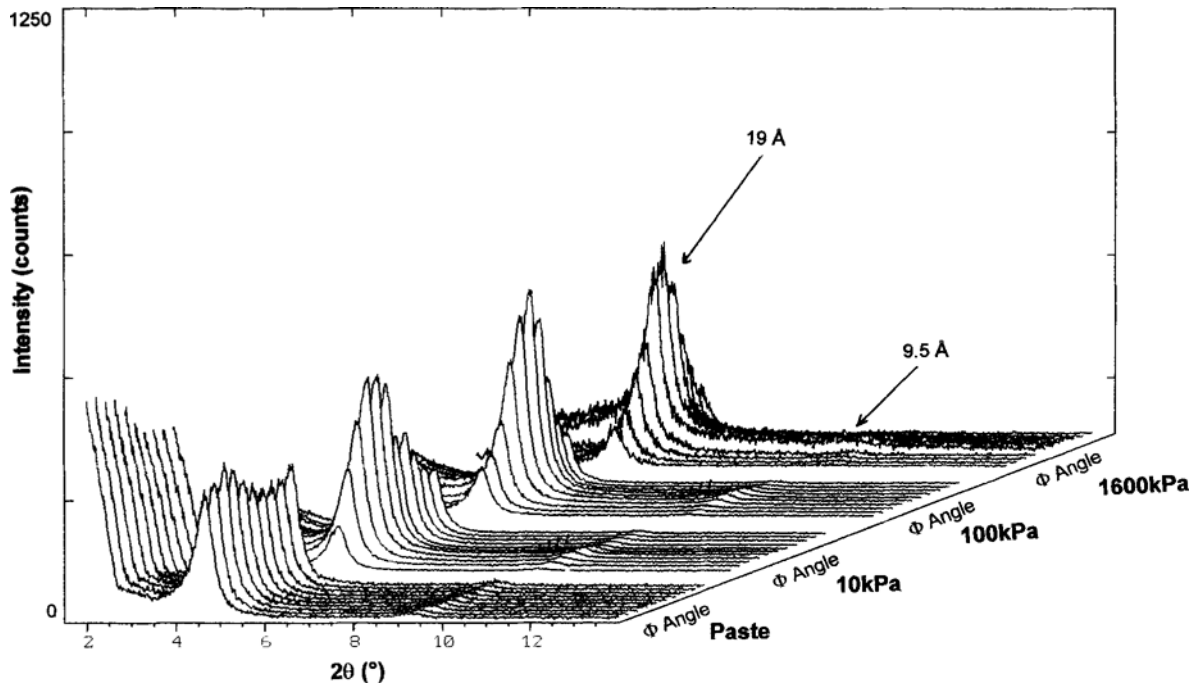


Figure 8. X-ray orientation patterns obtained on Wyoming montmorillonite on initial paste and for 10, 100, and 1600 kPa suction pressures.

of the particles increased as water content decreased, and we did not observe a reduction in orientation between 1.0–1.6 MPa. Note that, even at 32 kPa, the  $hk$  band corresponding to 020 and 0,2,11 from montmorillonite is intense (Figure 9). This result is in agreement with other data where a transmission device was used (Brindley and Brown, 1980).

#### Particle types

Only the observations made on clay pastes are reported here. Because Wyoming montmorillonite has been characterized elsewhere (Tessier and Pédro, 1987; Tessier, 1991), we refer to those results.

Saint Austell kaolinite is composed of crystallite aggregates, whose size is near 20,000 Å in width and with a thickness of 2000 Å (Figure 10a and 10b). The crystallite size of the (001) plane is ~1000 Å. Each crystallite is composed of ~100 layers which are often curved. The stacking of crystallites is approximately parallel.

The Salins clay fractions are characterized by very fine crystals, ~1000 Å in lateral dimensions and 100 Å thick, with a  $d(001)$  of 10 Å (Figure 10c). The packing of these small crystal units produces a randomly oriented clay matrix.

For the 0.2–2- $\mu\text{m}$  clay-size fraction of the La Bouzule clay large particles are present mainly made of crystal aggregates of illite, smectite, I-S, and kaolinite crystals (Figure 11a). The lateral dimensions of the (001) plane depended on their particle size (~2  $\mu\text{m}$ )

but thicknesses varied to ~1000 Å. These aggregates seemed to be flat, even if they contained many smectite layers. Inside the clay aggregates, small illite crystals (10 Å) and  $d(001)$  values at ~13 Å were observed. Distinctive kaolinite crystals and iron oxides (hematite) were also found (Figure 11b).

## DISCUSSION AND INTERPRETATION

#### Comparison of the diagrams

The 00 $l$  reflections of the different clays were grouped together to determine the evolution of the orientation, the 00 $l$  reflection, and an  $hk0$  reflection. For instance, in the orientation diagrams, the 001 and 020 reflections from La Bouzule (Figures 5, 6, and 7) were compared. Note that over the range of the highest water contents, *i.e.*, for low suction pressures, the relative intensities of the 00 $l$  and the  $hk$  bands are most different.

The 001 clay curves obtained (normalized surface area) at the same suction pressure (1.6 MPa) are superposed (Figure 12). In the La Bouzule clay, a very high intensity was obtained near the maximum orientation ( $\pi \sim 90^\circ$ ), whereas the diffracted intensity in Saint Austell kaolinite and Salins illite was much lower. For the La Bouzule clay-size fractions, the range of particle orientation was limited ( $\pm 40$ – $50^\circ$  relative to the horizontal plane). The most poorly oriented clay was the Wyoming montmorillonite.

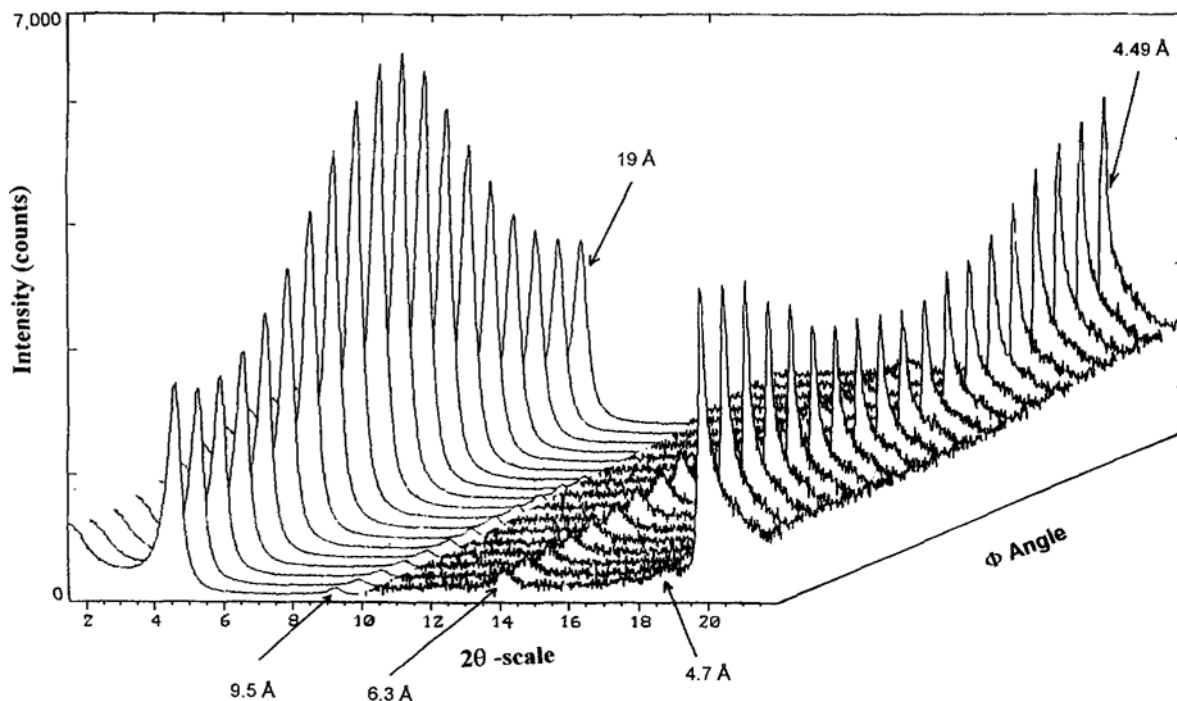


Figure 9. Comparison of the X-ray orientation patterns for 001 and  $hk$  reflections of Wyoming montmorillonite at 32 kPa.

#### Appearance of 001 reflections and intensity of $hk$ bands

Montmorillonite is the only clay studied with 001 reflections that may have a different position during drying. It is necessary to obtain  $\sim 5.0$  MPa to go from  $d(001)$  values with three  $H_2O$  layers (18.6 Å) to two  $H_2O$  layers (15.6 Å) (Tessier, 1984; Ben Rhaiem *et al.*, 1987) in Ca-rich montmorillonite. Our data indicate that, whatever the water content of the sample, kaolinite, Salins illite, and montmorillonite have a 001 diffraction peak. These three clays were relatively pure and have crystallites of significant size, which was confirmed by the specific-surface area data and TEM data. The number of layers in the coherent domains of Ca-rich montmorillonite is estimated at  $>8$  with face-to-face stacking of these coherent domains ( $\sim 50$  layers) (Tessier and Pédro, 1987; Touret *et al.*, 1990). In kaolinite, there were  $\sim 100$  layers per crystallite (Vasseur *et al.*, 1995) whereas, in illite, there were three to four layers, which is in agreement with the specific surface area (Djéran-Maigre *et al.*, 1998).

The results of the La Bouzule clay raises questions about the interpretation of patterns for material containing several clay types, especially with regard to the 001 and 020 reflections. Because the clays were Ca-saturated, unlimited swelling is not a reasonable explanation for the absence of the 001 reflection of smectite, and cation exchange will not affect kaolinite or illite. Different levels of organization, however, are

possible: (1) The La Bouzule clay is a mixture of several phases. Although kaolinite gives relatively intense diffraction peaks at high drying levels, the content in kaolinite in the La Bouzule clay is  $\sim 10\%$ . However, the kaolinite concentration in a highly hydrated clay decreases as water content increases. (2) In the wet sample where the particle arrangement is random, the number of measurable 001 reflections may be very small. For this clay, large aggregates are probably present with a very loose stacking separated by wide gaps (Figure 11). The size of the coherent domains must be small because the clay has a specific surface area similar to that of the Salins illite.

Hence, the conditions necessary to obtain the 001 reflection are not met in the La Bouzule clay prepared as a paste. In this case, the  $hk$  band and the 020 reflection, which are only slightly affected by environmental conditions, appear to be appropriate for studying orientation. On the other hand, drying produced a sufficiently compact and organized stacking so that the 001 reflection from kaolinite can be obtained.

#### Microstructure evolution

Water extraction from clay pastes is associated with particle rearrangement. The microstructure results from the evolution of the orientation of clay in the sample. The question is why orientation varies between clays and why particle orientations can change.



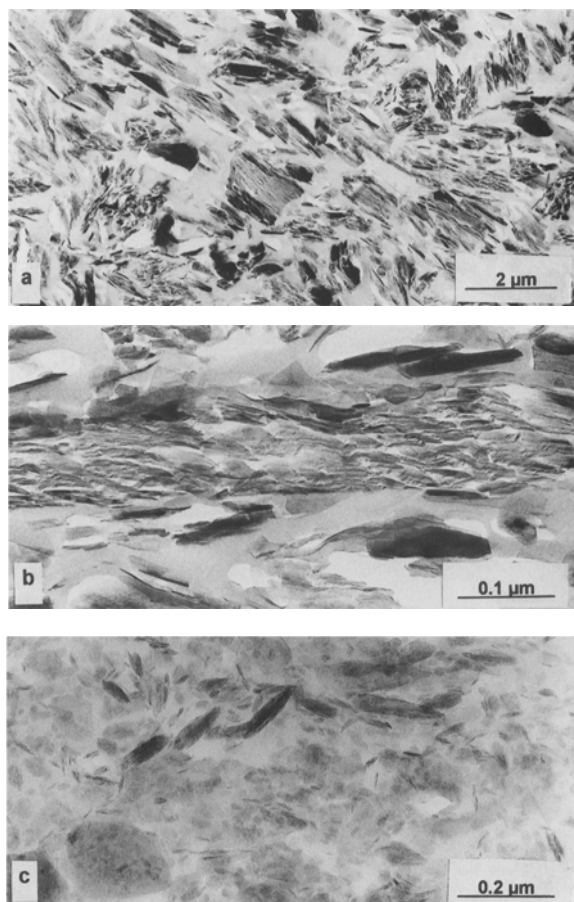


Figure 10. Microstructure of Saint Austell kaolinite (a and b), and of Salins illite (c).

Clays have different surface charges. In our experiments, kaolinite had a specific orientation compared to the other clays. The charge deficit of Saint Austell kaolinite layers is near zero and, at a pH close to neutrality, the basal faces of the crystallites have a charge close to neutrality (McBride, 1989). Thus, the hydrated structure of a kaolinite paste is extremely fragile. Clay in suspension or as a paste is oriented under the influence of gravity and water extraction. Aggregates, much larger than the crystallites which constitute them, consequently face each other.

Conversely, in montmorillonite, a permanent surface charge produces cohesion forces. TEM observations showed that particles mainly face one another, indicating the presence of a highly connected network (Tessier, 1991). In the absence of a suction force, this structure is isotropic (random grain orientations). A similar behavior was observed in the Salins illite and the La Bouzule clay, where the presence of 2:1 clay with a permanent charge deficit (illite-smectite) has a similar organization. However, because these clays are partially composed of illitic and kaolinitic particles,

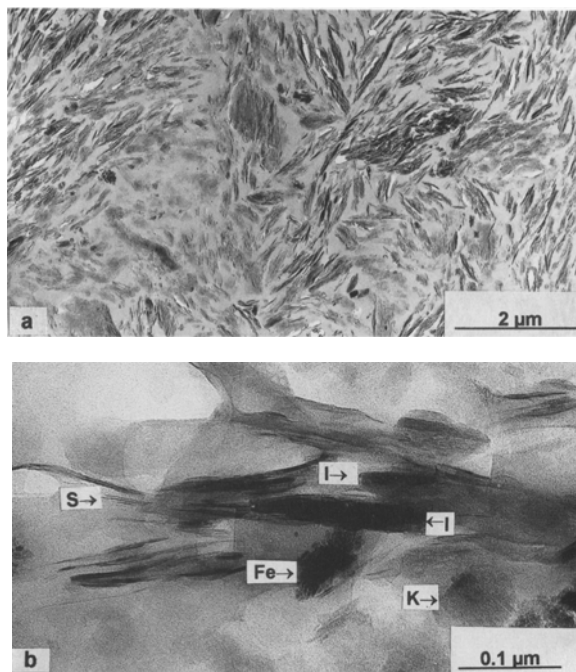


Figure 11. Microstructure of the La Bouzule clay (0.2–2 μm) with (a) general fabric, (b) presence of kaolinite (K), illite (I), and smectite (S) crystals, and iron oxides (Fe).

the network is more weakly connected. Although unstable, the structure is more stable than kaolinite. Clay-particle reorientation requires a given suction pressure. Note that the La Bouzule clay has the largest particle aggregates in the *xy* plane of the sample device ( $\leq 2$  or 2–5 μm), and this produces strongest orientation.

Clay orientation during drying is a phenomenon observed in all clays whereas the global disorientation of montmorillonite was observed at very high drying lev-

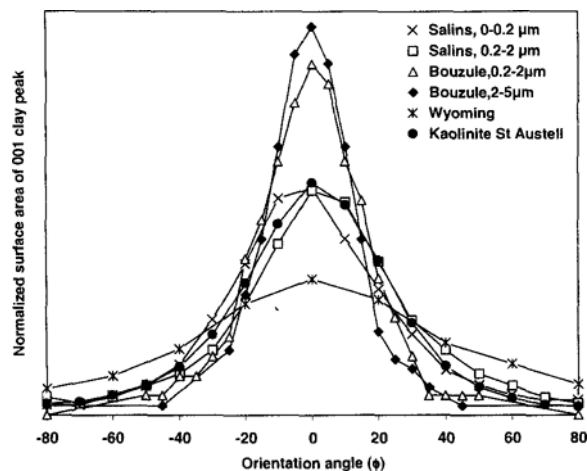


Figure 12. Superposition of the X-ray orientation curves obtained for the 001 reflection of the samples at 1600 kPa suction pressure after normalization.

els (~10 MPa) by Tessier (1978a). In the present study, disorientation occurs for kaolinite at ~1.6 MPa, when water contents close to the shrinkage limit (illites, kaolinites) were reached, or when the water outside the layers, in pores, became low (smectites). Our previous studies have shown that the shrinkage limit of Saint Austell kaolinite is near 1 bar (Tessier, 1984). Despite water desaturation of clay, the structure between the crystallites constituting the aggregates still reorganizes. We conclude that disorientation may occur between crystallites, although the clay has reached the shrinkage limit from a macroscopic point of view.

### CONCLUSIONS

Particle orientation, and thus changes in the microstructure, is a major factor characterizing clay during drying. This result was confirmed for non-swelling clays such as illite and kaolinite, as well as for swelling clays such as Wyoming montmorillonite. For the clays studied, the range of particle orientation depends on: (1) the clay aggregate (particle) extension (size) in the (001) plane, and (2) the crystal structure. Studying the orientation of hydrated particles by X-ray diffraction involves the effect of any change in the water content, solution composition, or the way in which the sample is mounted. The precise nature of the evolution of clay organization with respect to dehydration can be obtained by studying orientation.

Depending on the clay, either a 00 $l$  reflection, the 020 reflection, or an  $hkl$  band can be used to analyze orientation. In many cases the 020 reflection is most useful because the intensity of the peak is high and it appears to be independent of the water content and the degree of order in the stacking of layers along  $c$ .

The 00 $l$  reflections as a function of orientation require further analysis theoretically. The dilution ratio of clay in the presence of water and mixed with other clay phases requires consideration. Analysis should make it possible to determine the conditions required to obtain a sufficient symmetry in the distribution of orientations to obtain the 00 $l$  reflections. Such data may be used to develop organizational models of clays that consider more macroscopic structures than the basic 2:1 layers and their elementary stackings.

### ACKNOWLEDGMENTS

The senior author thanks the Spanish government for its support for his postdoctoral position at the INRA centre in Versailles and the INRA for providing work facilities.

### REFERENCES

Assouline, S., Tavares-Filho, J., and Tessier, D. (1997) Effect of compaction on soil physical and hydraulic properties: Experimental results and modeling. *Soil Science Society of America Journal*, **61**, 390–398.

Aylmore, L.A.G. and Quirk, J.P. (1959) Swelling of clay-water systems. *Nature*, **183**, 1752–1753.

Ben Rhaïem, H., Pons, C.H., and Tessier, D. (1987) Factors affecting the microstructure of smectites. In *Role of Cation*

*and History of Applied Stresses. Proceedings of International Clay Conference, Denver, Colorado* The Clay Minerals Society, Boulder, Colorado, 292–297.

Brindley, G.W. (1980) Order-disorder in clay minerals structures. In *Crystal Structures of Clay Minerals and Their X-ray Identification*, G.W. Brindley and G. Brown, eds., Mineralogical Society, London, 125–195.

Brindley, G.W. and Brown, G. eds. (1980) *Crystal Structures of Clay Minerals and Their X-ray Identification*. Mineralogical Society, London, 495 pp.

Courville, J., Tchoubar, D., and Tchoubar, C. (1979) Détermination expérimentale de la fonction d'orientation. Son application dans les calculs des bandes de diffraction. *Journal of Applied Crystallography*, **12**, 322–338.

Djéran-Maigre, I., Tessier, D., Grunberger, D., Velde, B., and Vasseur, G. (1998) Evolution of microstructures and of macroscopic properties of some clays during experimental compaction. *Marine and Petroleum Geology*, **15**, 109–129.

Elsass, F., Beaumont, A., Pernes, M., Jaunet, A.M., and Tessier, D. (1998) Changes in layer organization of Na- and Ca-exchanged smectite materials during solvent exchanges for embedment in resin. *The Canadian Mineralogist*, **36**, 1475–1483.

Grossman, R.B. and Millet, J.C. (1961) Carbonate removal from soils by a modification of the acetate buffer method. *Soil Science Society of America Proceedings*, **25**, 325–326.

Iñigo, A.C. and Tessier, D. (1996) Crystal structure and particle orientation in relation to behavior of clays during drying. *Advances in Clay Minerals*, 70–72.

Kim, J.M., Peacor, D.R., Tessier, D., and Elsass, F. (1995) A technique for maintaining texture and permanent expansion of smectite interlayer spacings for TEM observations. *Clays and Clay Minerals*, **43**, 51–57.

Kunze, G.W. and Rich, C.I. (1959) Mineralogical methods. In *Certain Properties of Selected Southeastern United States Soils and Mineralogical Procedures for Their Study*, C.I. Rich, L. Seatz, and F. Kunze, eds., Southern Cooperation Series Bulletin 61, 135–146.

Mamy, J. (1975) Les phénomènes de diffraction des rayonnements X et électroniques par les réseaux atomiques: Application à l'étude de l'ordre cristallin dans les minéraux argileux. *Annales Agronomiques*, **26**, 625–650.

McBride, M.B. (1989) Reactions controlling heavy metal solubility in soils. *Advances in Soil Science*, **10**, 1–56.

Méring, J. (1946) On the hydration of montmorillonite. *Transactions of the Faraday Society*, **42B**, 205–219.

Méring, J. (1949) L'interférence des rayons X dans les systèmes à stratification désordonnée. *Acta Crystallographica*, **2**, 371–377.

Nadeau, P.H., Wilson, M.J., McHardy, W.J., and Tait, J.M. (1984) Interstratified minerals as fundamental particles. *Science*, **225**, 923–925.

Norrish, K. (1954) The swelling of montmorillonite. *Discussions of the Faraday Society*, **18**, 120–134.

Plançon, A. (1980) The calculation of intensities diffracted by a partially oriented powder with a layer structure. *Journal of Applied Crystallography*, **13**, 524–528.

Pons, C.H., Rousseaux, F., and Tchoubar, D. (1981) Utilisation du rayonnement synchrotron en diffusion aux petits angles pour l'étude du gonflement des smectites: 1. Etude du système eau-montmorillonite-Na en fonction de la température. *Clay Minerals*, **16**, 23–42.

Reynolds, R.C. (1980) Interstratified clay minerals. In *Crystal Structures of Clay Minerals and Their X-ray Identification*, G.W. Brindley and F. Brown, eds., Mineralogical Society, London, 249–303.

Robert, M. and Tessier, D. (1974) Méthode de préparation des argiles des sols pour études minéralogiques. *Annales Agronomiques*, **25**, 859–882.

- Taylor, R.M. and Norrish, K. (1966) The measurement of orientation distribution and its application to quantitative X-ray diffraction analysis. *Clay Minerals*, **6**, 127–142.
- Tessier, D. (1978a) Étude de l'organisation des argiles calcaïques. Evolution au cours de la dessiccation. *Annales Agronomiques*, **29**, 319–355.
- Tessier, D. (1978b) Technique d'étude de l'orientation des particules argileuses utilisable sur des échantillons secs et humides. *Annales Agronomiques*, **29**, 193–207.
- Tessier, D. (1984) *Etude Expérimentale de l'Organisation des Matériaux Argileux: Hydratation, Gonflement et Structuration au Cours de la Dessiccation et de la Réhumectation*. INRA Versailles, France, 361 pp.
- Tessier, D. (1991) Behavior and microstructure of clay minerals. In *Soil Colloids and Their Associations in Aggregates*, M.F. De Boodt, M. Hayes, and A. Herbillon eds., NATO Book Series, Plenum Publishing Corporation, New York, 387–415.
- Tessier, D. and Pédro, G. (1976) Les modalités de l'organisation des particules dans les matériaux argileux. Evolution des principales argiles Ca au cours du phénomène de retrait. *Science du Sol*, **2**, 85–99.
- Tessier, D. and Pédro, G. (1987) Mineralogical Characterization of 2:1 Clays in Soils: Importance of the Clay Texture. In *Proceedings of the International Clay Conference, Denver, 1985*, L.G. Schultz, H. van Olphen, and F.A. Mumpton, eds., The Clay Minerals Society, Bloomington, Indiana, 78–84.
- Tessier, D., Bouzigues, J.C., Favrot, J.C., and Valles, V. (1992) Influence du micro-relief sur l'évolution texturée dans les sols lessivés de la vallée de la Garonne. Différenciation des structures vertique et prismatique. *Comptes Rendus Académie Sciences Paris*, **315**, 1027–1032.
- Touret, O., Pons, C.H., Tessier, D., and Tardy, Y. (1990) Etude de la répartition de l'eau dans des argiles saturées  $Mg^{2+}$  aux fortes teneurs en eau. *Clay Minerals*, **25**, 217–233.
- Vasseur, G., Djéran-Maigre, I., Grunberger, D., Rousset, G., Tessier, D., and Velde, B. (1995) Evolution of structural and physical parameters of clays during experimental compaction. *Marine and Petroleum Geology*, **12**, 941–954.
- Wiewiora, A. (1982) Oblique-texture method in transmission X-ray diffractometry of clays and clay minerals. In *Proceedings of the 9th Clay Mineralogy and Petrology Conference, Zvolen-Praha, Czechoslovakia*, 43–51.
- Wiewiora, A. and Weiss, Z. (1985) X-ray powder transmission diffractometry determination of mica polytypes: Method and application to natural samples. *Clay Minerals*, **20**, 231–248.
- Wilding, L. and Tessier, D. (1988) Genesis of vertisols: Shrink-swell phenomena. In *Vertisols: Their Distribution, Properties, Classification and Management*, L. Wilding and R. Puentes, eds., Texas A & M University, Texas 55–81.
- E-mail of corresponding author: tessier@versailles.inra.fr  
(Received 17 April 1998; accepted 5 July 2000; Ms. 98-052)